JOURNAL OF VIROLOGY, Oct. 1980, p. 1-17
0022-538X/80/10-0001/17$02.00/0

Vol. 36, No. 1

Correlation Between Genetic Map and Map of Cleavage Sites for Sequence-Specific Endonucleases *Sal*I, *Kpn*I, *Bgl*I, and *Bam*HI in Bacteriophage T4 Cytosine-Containing DNA

KARIN CARLSON

Institute of Medical Biology, University of Tromsø, 9001 Tromsø, Norway

Cleavage sites for *Sal*I, *Kpn*I, *Bgl*I, and *Bam*HI in cytosine-containing DNA from T4 *alc*10(*alc*) *nd*28(*den*A) *D2a*2(*den*B) *am*E51x5(*56*) *am*N55x5(*42*) have been mapped relative to each other, and the positions of deletions *sa*Δ9(*D1-stp*), *r*1589(*r*II), *del*(*39-56*)12, and *tk*2(*r*I-*tk*) relative to these cleavage sites have been determined. Based on these analyses, a physical map of the T4 genome containing 166 kilobase pairs has been constructed.

Recent studies from this (4) and other (14, 21, 30) laboratories have yielded cleavage maps of cytosine-containing DNA from bacteriophage T4 for several sequence-specific endonucleases (restriction enzymes). The potential value of these maps, of course, hinges on the accuracy with which the genetic content of each fragment is known.

Deletion mutants of T4 may be utilized to establish directly the correlation between genetic and physical maps, since their genetic deficiencies can be compared with the altered cleavage patterns of their DNA. This paper presents a cleavage map for T4 DNA constructed with the enzymes *Sal*I, *Kpn*I, *Bgl*I, and *Bam*HI and its correlation to the genetic map of the phage genome based on an analysis of deletion mutants.

Correlations between restriction cleavage maps and the genetic map of T4 have been derived independently by O'Farrell et al. (P. O'Farrell, E. Kutter, and M. Nakanishi, manuscript in preparation) and by R. Marsh (manuscript in preparation) by different methods.

MATERIALS AND METHODS

Strains. (i) Phage. The phage strains employed in this study are listed in Table 1, and the construction steps leading up to strains Cyt-9,1589, Cyt-9,12, and Cyt-9,*tk*2 are summarized in Table 2.

Relevant genotypes were verified as follows. **(a)** ***alc***$^-$ ***den***A$^-$ ***den***B$^-$ ***am*** **dCTPase**$^-$ **("Cyt phenotype").** Phage stocks prepared in *Escherichia coli* B834, which is *sup*^{0} *hsd*, will plate on *E. coli* B834, but not on *E. coli* B23, which is *sup*^{0} *hsd*$^+$ (23).

(b) "*r*H23" (*r*II$^-$). There is no growth in *E. coli* K803(λ) and no complementation or marker rescue in K803(λ) of *r*II point mutants; it is resistant to acriflavine (10 μg/ml in LB). "*r*H23" is not identical to the original *r*H23; it contains a longer deletion extending from *r*II into *ac* (T. J. Snopek and R. E. Depew, cited in reference 16).

(c) *r*1584 (*r*II$^-$). There is complementation or marker rescue in K803(λ) of certain *r*II point mutants. The complementation or marker rescue pattern was the same as that which we observed with the original T4B *r*1589 strain.

(d) *del*(*39-56*)12. There is no growth in *E. coli* CTr5x (12). All other phage strains employed in this study grow in CTr5x.

(e) Amber mutations in essential genes. There is no complementation in *E. coli* B23, which is *sup*^{0}, to the same single *am* mutant of T4.

(f) *tk*2 (*r*I$^-$). There are r plaques on *E. coli* K803. *r*II$^-$ phage give r plaques on B strains of *E. coli* only (3).

The presence or absence of the *o* allele, which confers resistance to osmotic shock, was not tested.

(ii) Bacteria. *E. coli* B834, which is *sup*^{0} *hsdR hsdM* (31), and K803, which is *sup-2 hsdR hsdM rgl* (31), were from E. Kutter. *E. coli* B23, which is *sup*^{0} *hsd*$^+$, was from A. W. Kozinski. Strain K803(λ) was constructed in this laboratory. Strain CTr5x (8) was obtained from T. J. Snopek.

(iii) Growth of strains. Bacteria and phage were grown in LB (1) and plated on tryptone agar containing the following (per liter): tryptone (Difco Laboratories), 10 g; NaCl, 8 g; glucose·H_2O, 1.1 g; 1 M NaOH, 1.25 ml; and agar (Difco), 11 g (bottom) or 6.5 g (top). All phage were propagated in K803, and the same strain was used for phage crosses. Phage with cytosine-containing DNA were obtained after one cycle of growth in B834. DNA was prepared by phenol extraction of CsCl-purified phage, followed by exhaustive dialysis of the DNA against 10 mM NaCl-10 mM Tris-hydrochloride, pH 7.4.

Isotopes and chemicals. α-^{32}P-labeled deoxyribonucleotide triphosphates were obtained from Amersham Ltd. (specific activity, 2,000 to 3,000 Ci/mmol); all four deoxyribonucleotide triphosphates were used interchangeably. Agarose, acrylamide, and bisacrylamide were from Bio-Rad Laboratories (catalog no. 162 0100, 161 0101, and 161 0201, respectively). Sephadex G-50 and Blue Dextran 2000 were from Pharmacia Fine Chemicals. Tris was from Fisher Scientific Co. (catalog no. T395). Unlabeled deoxyribonucleotide triphosphates were from PL Biochemicals. Formamide

(Merck catalog no. 9684) was recrystallized twice before use. Other chemicals were standard analytical grade.

Enzymes. Endonucleases *Sal*I, *Kpn*I, and *Bam*HI were obtained and assayed as described previously (4). *Bgl*I was purchased from New England Biolabs and assayed in the same manner as *Sal*I. *E. coli* DNA polymerase I (EC 2.7.7.7) was from Boehringer Mannheim Corp. (catalog no. 104 485).

Electrophoresis. Agarose gel electrophoresis was carried out as described previously (4). Acrylamide gels contained 8% acrylamide and 0.27% bisacrylamide in 50% glycerol–45 mM Tris-borate (pH 8.3)–1.2 mM Na_2EDTA (20). They were 12 by 15 by 0.15 cm and were run vertically for 5 h at 180 V and 28 mA.

Upon the conclusion of electrophoresis, gels were stained with ethidium bromide and photographed. Film negatives were scanned in a Transidyne densitometer, and the distance from the point of application to each band was determined. Sizes of reference fragments in kilobase pairs (kbp) were plotted against the inverse of the distance migrated (25). These plots could be approximated with straight lines up to about 20 kbp. Sizes of unknown fragments were obtained by interpolation on the standard curve.

Labeling of DNA fragments. DNA fragments, eluted from agarose gels as described previously (4), were labeled by nick translation (17) in a final volume of 100 μl, using three unlabeled deoxyribonucleotide triphosphates each at 1.8 μM, 50 μCi (about 0.02 μM) of the fourth α-^{32}P-labeled deoxyribonucleotide triphosphate, 50 mM Tris-hydrochloride (pH 7.8), 5 mM $MgCl_2$, 10 mM β-mercaptoethanol, 5 U of *E. coli* DNA polymerase I, and 0.001 μg of pancreatic DNase I. The amount of DNA was too low for an accurate estimation, but was probably in the range of from 0.05 to 0.5 μg. The reaction was allowed to proceed for 4 h at 15°C. A 20-μl amount of Blue Dextran 2000 in 50 mM Tris-hydrochloride (pH 8.0)–1 mM Na_2EDTA was added, and the mixture was passed over a column (7 by 0.5 cm) of Sephadex G-50 in 50 mM Tris-hydrochloride (pH 8.0)–1 mM Na_2EDTA. The excluded fractions, containing the Blue Dextran 2000, were collected for analysis.

Hybridization. Fragment DNA was denatured and transferred from agarose slabs to nitrocellulose membrane filters (type HAWP; Millipore Corp.), using the following modification suggested by E. Southern of the Southern procedure (24). Gels were soaked in freshly prepared 0.1 M NaOH–1.5 M NaCl (pH 12.6) for 30 min, rinsed in doubly distilled water, soaked in 3 M sodium acetate (pH 5.5) for 40 min, again rinsed in doubly distilled water, and then blotted overnight onto the membrane filter with 20× SSC (1× SSC is 0.15 M NaCl plus 0.015 M sodium citrate) as the conveying liquid. Filters were rinsed in doubly distilled water, dried at room temperature, and baked in vacuo for 2 h at 80°C. This resulted in a reproducible transfer of DNA in the size range from 2 to 15 kb. Filters were then incubated in a solution containing 0.01% sodium lauryl sulfate and 0.2% each polyvinylpyrrolidone, bovine serum albumin, and Ficoll (7) in 6× SSC for 4 to 6 h at 67°C, rinsed in doubly distilled water, and cut into strips for hybridization.

TABLE 1. *Phage strains employed in this study*

Phage strain	Abbreviated notation	Source
T4D "*r*H23"x4(*r*II-*ac*)[a]		E. Kutter (16)[b]
T4B *r*1589(*r*II)		P. Snustad (6)
T4D *r*1589(*r*II) *del*(*39-56*)12		G. Mosig (12)
T4D *am*E51x5(*56*)		J. Wiberg
T4D *o tk*2(*r*I-*tk*)		D. H. Hall (5)
T4D *alc*10(*alc*) *nd*28(*den*A) *D2a*2(*den*B) *am*E51x5(*56*) *am*N55x5(*42*)	Cyt-0	J. Wiberg (stock no. JW819)
T4D *alc*2(*alc*) *nd*28(*den*A) *saΔ*9(*D1-stp*) *am*E51(*56*)[a]	Cyt-9	E. Kutter
T4D *alc*2(*alc*) *nd*28(*den*A) *saΔ*9(*D1-stp*) *r*1589(*r*II) *am*E51(*56*)[a]	Cyt-9,1589	This study
T4D *alc*2(*alc*) *nd*28(*den*A) *saΔ*9(*D1-stp*) *am*E51(*56*) *del*(*39-56*)12	Cyt-9,12	This study
T4D *alc*2(*alc*) *nd*28(*den*A) *saΔ*9(*D1-stp*) *am*E51(*56*) *tk*2(*r*I-*tk*)	Cyt-9,*tk*2	This study

[a] Deletions *saΔ*9 and "*r*H23" also inactivate *den*B.
[b] Backcrossed here.

TABLE 2. *Construction of Cyt-9,1589, Cyt-9,12, and Cyt-9,tk2*

Cross no.	Parental phages		Selected recombinant
	1	2	
1	Cyt-9	*r*1589 *del*(*39-56*)12	Cyt-9,1589
2	*am*E51x5	"*r*H23"x4	"*r*H23"x4 *am*E51x5
3	*am*E51x5	*r*1589 *del*(*39-56*)12	*del*(*39-56*)12 *am*E51x5
4	"*r*H23"x4 *am*E51x5	*del*(*39-56*)12 *am*E51x5	"*r*H23"x4 *del*(*39-56*)12 *am*E51x5
5	Cyt-9	"*r*H23"x4 *del*(*39-56*)12 *am*E51x5	Cyt-9,12
6	*am*E51x5	*o tk*2	*am*E51x5 *tk*2
7	Cyt-9	*am*E51x5 *tk*2	Cyt-9,*tk*2

Hybridization of labeled DNA to these strips was carried out in plastic sealable cooking bags in about 8 to 10 ml of a solution containing 50% formamide, 2× SSC, 2.5 mM NaP_i (pH 7.7), and 10^4 to 10^6 cpm of labeled, sonicated, and heat-denatured DNA for 18 h at 42°C. The filters were washed in three changes of 2× SSC for 2 h each at 42°C, rinsed in doubly distilled water, and autoradiographed (Kodak Autoprocess film, catalog no. 300 3688).

Hybridized DNA was removed by treating the filters with 0.1 M NaOH–1.5 M NaCl (pH 12.6), followed by 3 M sodium acetate (pH 5.5). The filters were then rinsed in doubly distilled water and dried. Some bound DNA was lost during this treatment, but the filters could be reused several times for hybridization.

RESULTS

Fragmentation of Cyt-0 DNA. The mutations *nd*28, *D2a*2, *am*E51, and *am*N55 in phage strain Cyt-0 are all point mutations. The cleavage of Cyt-0 DNA by *SalI*, *KpnI*, and *BglI*, as well as by combinations of these enzymes, is shown in Fig. 1. Electrophoresis of the *SalI* cleavage product yielded eight bands, one being a doublet containing two fragments (see below). *KpnI* and *BglI* cleavages of Cyt-0 DNA upon electrophoresis yielded seven bands each, each band corresponding to a single fragment. The double digests *SalI* + *KpnI*, *SalI* + *BglI*, and *KpnI* + *BglI* yielded 15, 15, and 14 bands, respectively. In each of the two former cleavages, 1 of the 15 bands was a doublet, as shown elsewhere (reference 4 and see below), so that the number of *SalI* + *KpnI* fragments and of *SalI* + *BglI* fragments was 16.

The lengths of the fragments were calculated from their electrophoretic mobility. As length standards, restriction fragments from either phage λ DNA (11, 19, 29), T4 Cyt-9 DNA cleaved with *SalI* + *KpnI* (4), or phage P4 DNA (10, 13) were used. The latter standard was used to estimate sizes of fragments 3 kbp and smaller. All values were normalized to a length of λ DNA equal to 48.3 kbp (26).

All fragments obtained from Cyt-0 DNA were named in order of decreasing size, single digest fragments by letters and double digest fragments by numbers. Since further analysis (see below) allowed the determination of separate sizes for the two fragments in the *SalI* doublet, those two fragments were named C and D according to their size. Since it was not known which fragment was the larger in the *SalI* + *KpnI* doublet or in the *SalI* + *BglI* doublet, those are referred to as SK-11a and SK-11b, and SB-9a and SB-9b, respectively (abbreviations used: *KpnI*, endo R·*KpnI*; *BglI*, endo R·*BglI*; *SalI*, endo R·*SalI*; S-G, etc., fragment T4 *SalI*-G, etc.; K-G, etc., fragment T4 *KpnI*-G, etc.; B-G, fragment T4 *BglI*-G, etc.; SK-5, etc., fragment 5, etc., from a mixed digest of T4 DNA with *SalI* + *KpnI*; SB-5, etc., fragment 5, etc., from a mixed digest of T4 DNA with *SalI* + *BglI*; KB-5, etc., fragment 5, etc., from a mixed digest of T4 DNA with *KpnI* + *BglI*). The length estimates are shown in Table 3. The designations of *SalI* fragments (and of *SalI* + *KpnI* fragments) differ from the previous designations (4), since Cyt-0 contained one more *SalI* site in addition to those found in Cyt-9, which was used in the previous study (4). A comparison of Fig. 2A here and Fig. 1 in reference 4 will show the correspondence between the two nomenclatures.

Fragmentation of DNA carrying different deletions. To locate the cleavage sites with respect to the genetic map, several phage strains carrying different deletions which are genetically characterized and mapped were used. Figure 2 and Table 4 show the cleavage patterns observed with DNA from these mutants.

(i) Cyt-9 DNA. Cyt-9 DNA (Fig. 2A) differed from Cyt-0 DNA in carrying the *saΔ*9 deletion in the *D2* region (9), carrying *alc*2 instead of *alc*10, and carrying wild-type gene *42*.

A comparison of Fig. 2A and 1C shows that a *SalI* site present in Cyt-0 DNA was missing in Cyt-9 DNA, confirming earlier observations by Takahashi et al. (28). Fragment S-F and one fragment from the S-C/D doublet were replaced by a fusion fragment migrating between S-A and S-B, rather near S-B. It will be shown below that this fusion fragment contained S-C and S-F.

One *KpnI* fragment (K-E) and one *BglI* fragment (B-F) were reduced in size. The difference in size corresponded to about 2.5 kbp (Table 4). The 2.5 kbp were attributed to *saΔ*9, which placed this deletion across the *SalI* cleavage site between C and F and within fragments K-E and B-F.

Except for the differences noted above, the cleavage pattern with all combinations of enzymes was the same for Cyt-0 and Cyt-9 DNAs. It was concluded that the somewhat different genotype of these strains outside *saΔ*9 did not significantly alter the cleavage pattern for these enzymes. Thus, the dCTPase deficiency caused by the *am*E51 mutation allowed as good cytosine substitution in the phage DNA in the areas recognized by these enzymes as did the deficiencies in dCTPase (EC 3.6.1.12) (*am*E51x5) and dCMP HMase (EC 2.1.2.8) (*am*N55x5) together.

(ii) Cyt-9,1589 DNA. Phage strain Cyt-9,1589 (Fig. 2B) carried the *r*II deletion *r*1589, which spans the end of *r*IIA and the beginning of *r*IIB (6), thus deleting the *r*IIA/*r*IIB border commonly used as the zero point in genetic mapping (32). In addition, strain Cyt-9,1589 car-

ried the same mutations as did strain Cyt-9. The analysis in Fig. 2B in comparison with that in Fig. 2A shows that the *Sal*I fusion fragment created by the *sa*Δ9 deletion migrated closer to S-B. Fragment K-E migrated slightly further down in the gel. The cleavage site between B-B and B-F was removed, fusing those two to a large fragment in the area of B-A. Accordingly, deletion *r*1589 lay within K-E, within S-C or S-F, and across the junction between B-B and B-F.

(iii) Cyt-9,12 DNA. Phage strain Cyt-9,12 (Fig. 2C) carried a long deletion in the region between genes *39* and *56* (12), in addition to the mutations in strain Cyt-9. The *Sal*I pattern (tracing a), in comparison with the pattern obtained from DNA carrying only the *sa*Δ9 deletion but not *del*(*39-56*)12 (Fig. 2B, tracing a), shows that the S-(C+F) fusion fragment created by the *sa*Δ9 deletion was shortened and comigrated with the S-D fragment, creating a new doublet in this position. Tracing b shows that K-E and K-G were missing. To be sure to detect the K-G fragment, if it were present, the gel was slightly overloaded, and the three large fragments, therefore, did not form separate bands. No fusion fragment was visible in the area between K-D and K-E, showing that both sites surrounding K-G must be deleted and that K-E must be fused to the next *Kpn*I fragment on the other side of K-G. The *Bgl*I pattern (tracing c) shows a shortening of fragment B-B. Deletion (*39–56*)12, therefore, lay within B-B and S-(C+F), spanning the two *Kpn*I sites separating K-G from its neighbors.

(iv) Cyt-9,*tk*2. Phage strain Cyt-9,*tk*2 (Fig. 2D) carried a deletion eliminating *r*I and *tk* functions (5) in addition to the Cyt-9 mutations. The S-(C+F) fusion fragment was seen in its original position between S-A and S-B (Fig. 2B, tracing a). The S-D and S-E fragments were missing, and in their place a new fusion fragment was seen between S-B and the original position of S-C/D. The *Kpn*I pattern shows that either K-B or K-C was shortened. These fragments migrated very closely together, so that it is difficult to determine which of the two is seen in Fig. 2D, tracing b. A subsequent analysis (see below) indicated that the deletion *tk*2 was within fragment K-B. The new fragment migrated between the original position of K-C and K-D. Fragments B-D and B-E were fused to a new fragment migrating between B-B and B-C. These results placed the deletion *tk*2 within K-B or K-C, spanning the sites between *Bgl*I-D and -E and between *Sal*I-D and -E.

The results obtained from cleavage of DNA containing deletions *sa*Δ9, *r*1589, *del*(*39-56*)12, and *tk*2 with *Sal*I, *Kpn*I, and *Bgl*I alone (Fig. 2) or in combinations (data not shown) are summarized in Table 4. Table 4 also shows the lengths of the deletions calculated from the changes in electrophoretic mobility.

Location of cleavage sites. The order of *Kpn*I and *Sal*I fragments from Cyt-9 DNA with respect to each other was determined previously (4; as noted above, the *Sal*I fragments were renamed here due to the presence of an additional *Sal*I site in Cyt-0 DNA), with two ambiguities: the order of *Sal*I fragments within K-C and the order of *Kpn*I fragments within S-(C+F). The small K-G fragment was inadvert-

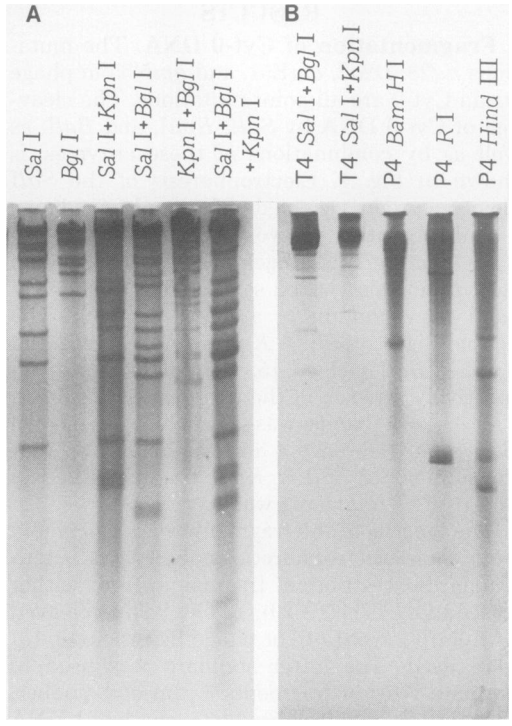

FIG. 1 A and B. *Agarose (A and C) and polyacrylamide (B) gel electrophoresis of T4 Cyt and P4 DNAs. (A) Cleavage of Cyt-0 DNA by SalI, KpnI, and BglI, alone and in combinations. (B) Cleavage of T4 Cyt-9,1589 DNA and of P4 DNA. The T4 bands are as follows (top to bottom): slot 1—SB-11, SB-13, SB-14, and SB-15; slot 2—SK-12, SK-13, and SK-15. Fragments SB-12 and SK-14 are absent in Cyt-9,1589 digests (Table 4). Electrophoresis in (A) and (B) is from top to bottom. (C) Cleavage of Cyt-0 DNA; densitometer tracings of negatives from photographs of gels like the one shown in (A). Electrophoresis direction is from left to right. Tracings from top to bottom: a, SalI; b, KpnI; c, BglI; d, SalI + KpnI; e, SalI + BglI; f, KpnI + BglI. Fragments are named in order of decreasing length, single digest fragments by letters and double digest fragments by numbers. The smallest fragment, SB-15, is not included. The unmarked peak near the top of the gel consists of undigested or partially digested DNA.*

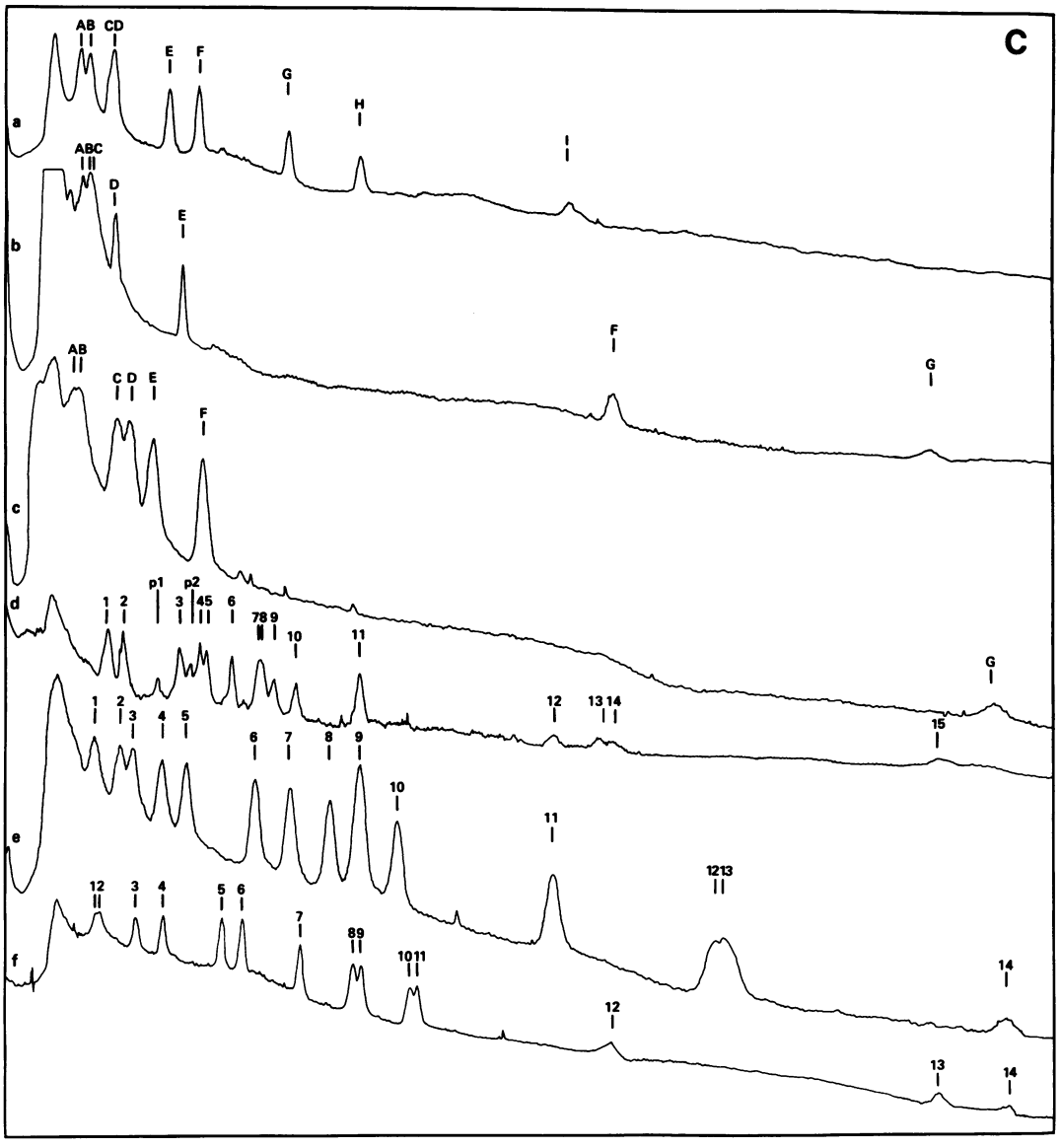

FIG. 1C.

ently overlooked previously; it was obtained from all strains except Cyt-9,12.

The order of the *SalI* fragments I and G within K-C was derived by assignment of a partially cleaved SK fragment (4). Neither S-I nor S-G was cleaved by *BglI* (or *Bam*HI). The ambiguity within K-C, therefore, could not be further resolved here. Rüger et al. (21), however, have derived the same order of *SalI* fragments as I have.

As shown in Fig. 2C, fragment K-G was adjacent to K-E. Having accidentally overlooked K-G, we previously assigned K-F to this position to account for a partially cleaved *KpnI* fragment (4). K-F, however, was obtained from Cyt-9,12 and, therefore, must be located elsewhere (see below). Since K-E contained *sa*Δ9 and *r*1589 (Fig. 2A and B) and K-G lay under *del*(*39-56*)12 (Fig. 2C), the clockwise order of *KpnI* fragments in this region must be D-E-G-C.

The *SalI* + *KpnI* map may be aligned with the genetic map based on the analyses of DNA from the deletion mutants in Fig. 2 and Table 4 (the completed map is shown in Fig. 8). The deletion analysis also gives the approximate locations of *BglI* fragments B, D, E, and F. To

TABLE 3. *Approximate sizes of T4 restriction fragments from electrophoretic mobility*

Fragment	Approx size (kbp) ± standard deviation[a]					
	Single digests			Double digests		
	*Sal*I	*Kpn*I	*Bgl*I	*Sal*I + *Kpn*I	*Sal*I + *Bgl*I	*Kpn*I + *Bgl*I
A	~40	~50	~50			
B	~33	~40	~40			
C		~36	23.5 ± 0.97 (9)			
C/D	24.1 ± 1.0 (6)					
D		23.9 ± 0.33 (10)	21.4 ± 1.0 (7)			
E	15.0 ± 0.68 (6)	14.5 ± 0.39 (10)	17.8 ± 0.77 (8)			
F	13.0 ± 0.78 (4)	3.2 (2)	13.2 ± 0.28 (6)			
G	8.9 ± 0.27 (6)	1.5 (2)	1.0 (1)			
H	7.0 ± 0.25 (6)					
I	3.9 ± 0.33 (6)					
1				26.0 ± 2.6 (4)	~32	~34
2				22.6 ± 0.84 (4)	23.8 ± 0.83 (9)	~31
3				14.7 ± 0.88 (4)	21.2 ± 0.56 (6)	21.3 ± 1.3 (4)
4				13.2 ± 0.44 (4)	16.8 ± 0.34 (8)	17.6 ± 0.84 (4)
5				12.8 ± 0.33 (4)	14.3 ± 0.53 (8)	12.7 ± 0.43 (4)
6				11.6 ± 14.4 (4)	10.2 ± 0.41 (8)	11.4 ± 0.39 (6)
7					8.8 ± 0.25 (7)	8.8 ± 0.49 (5)
7/8				10.4 ± 0.39 (4)		
8					7.6 ± 0.35 (10)	7.2 (2)
9				9.9 ± 0.38 (4)	6.9 ± 0.20 (9)	7.1 (2)
10				8.9 ± 0.27 (4)	6.1 ± 0.30 (9)	5.9 ± 0.47 (6)
11				7.0 ± 0.35 (4)	3.9 ± 0.31 (9)	5.5 ± 0.2 (2)
12				3.8 ± 0.67 (4)	2.8 ± 0.16 (3)	3.3 (1)
13				3.2 (2)	2.6 ± 0.2 (2)	1.6 ± 0.1 (2)
14				3.1 (2)	1.2 ± 0.03 (2)	1.1 (1)
15				1.6 (1)	0.8 (1)	

[a] Number of determinations is given within parentheses.

ascertain these positions and locate the remaining fragments, double digests, reciprocal digests, and hybridizations were performed.

(i) *Bam*HI cleavage. *Bam*HI cleaves T4 Cyt DNA once (28, 30). Figure 3 shows the cleavage patterns obtained with *Bam*HI together with *Sal*I, *Kpn*I, or *Bgl*I (substrate Cyt-0 DNA). A comparison of Fig. 3 and 1 shows that the *Bam*HI site lay within S-A, yielding new fragments of ~28 kbp (between S-B and S-C/D) and 12.2 kbp (between S-F and S-G); within either K-A, K-B, or K-C, yielding a short new fragment of about 1.8 kbp (just above K-G); and within B-C, yielding new fragments of 17.5 kbp (comigrating with B-E) and 5.3 kbp (below B-F).

(ii) *Kpn*I cleavage. The analysis in Fig. 2 showed that K-G was located between K-E and K-C. This was further confirmed by hybridizing labeled K-G to *Sal*I + *Bgl*I fragments of Cyt-0 DNA: K-G hybridized to fragment SB-3, which contained part of B-B and of S-C (Table 4 and see below) (data not shown). The position of K-F and the allocation of SK-13 and SK-14 remained unclear. Figure 4 shows hybridization of these fragments to blots of T4 Cyt-0 DNA. Fragment K-F hybridized to SB-2. Fragments SK-13 and SK-14 were difficult to separate from each other, since they migrated closely together (Fig. 1A and C). The analyses in Fig. 4b (predominantly SK-13) and Fig. 4c (predominantly SK-14) suggest that SK-13 was identical to K-F, hybridizing within SB-2 (= B-C [Fig. 5A]), whereas SK-14 hybridized to SB-6. Digestion of isolated B-C with *Kpn*I yielded fragments KB-5, KB-8, and KB-12 (= K-F) (data not shown). These analyses placed K-F between K-B and K-A. Fragment S-A, therefore, contained K-F (SK-13) in addition to SK-2 and SK-4 (4). S-A is the largest *Sal*I fragment, and its size cannot be determined precisely from its electrophoretic mobility, which explains why the error went undetected.

(iii) *Bgl*I cleavage. Results from reciprocal digestion of *Bgl*I fragments with *Sal*I and of *Sal*I fragments with *Bgl*I are shown in Fig. 5. Figure 5A shows that the mixture of B-A and B-B yielded SB-1, SB-3, SB-7, SB-8, SB-9, SB-11, and SB-13. B-C was not cleaved by *Sal*I and corresponded to SB-2. B-D yielded SB-5 and SB-10, B-E yielded SB-4, and B-F yielded SB-6 and SB-12. Fragment B-G was analyzed by hybridization (Fig. 6). This fragment, which was

TABLE 4. *Location and size of T4 deletions*

Deletion	Fragments affected	Net loss[a]	Avg loss[b]
*sa*Δ9	S-C and S-F	2.7	
	K-E	2.3	
	SK-6 and SK-14	2.3	
	B-F	2.7	
	SB-6 and SB-12	2.7	2.5 ± 0.2
*r*1589	B-B and B-F	ND[c]	
	S-(C+F)	ND	
	K-E	0.89	
	SB-3 and SB-(6+12)	ND	
	SK-(6+14)	1.0	
	KB-7 and KB-11	ND	0.9
*del(39-56)*12	S-(C+F)	10.9	
	B-B	ND	
	SB-3	11.1	11.1
*tk*2	S-D and S-E	9.6	
	K-B	10.3	
	SK-3 and SK-7	ND	
	B-D and B-E	9.4	
	SB-4 and SB-5	10.1	9.9 ± 0.4

[a] Difference in kbp between the lengths of fragments with and without the respective deletions.
[b] Average in kbp ± standard deviation.
[c] ND, Not determined.

identical to SB-14, hybridized to S-A, and to SK-2 which contained the common part of S-A and K-A. Fragment SB-15 was not recovered in the reanalysis, presumably due to its small size. B-E and SB-4 were close in size, but not identical. SB-15 was, therefore, attributed to B-E, adjacent to SB-4.

The corresponding digests of *SalI* fragments with *BglI* (Fig. 5B) show that S-A yielded SB-2, SB-8, SB-10, and SB-14. S-B was not cleaved by *BglI* and corresponded to SB-1. S-C/D yielded SB-3, SB-4, SB-9, andB-12. S-E yielded SB-5, and S-F yielded SB-6 and SB-13, whereas S-G, S-H, and S-I were not cleaved by *BglI* (they corresponded to SB-7, SB-9, and SB-11, respectively [data not shown]). Fragment SB-15 was not recovered in the reanalysis of *SalI* fragments by *BglI* cleavage. There was a small size difference between S-E and SB-5. SB-15 was, therefore, attributed to S-E, which accordingly contained SB-5 and SB-15.

Bands in the position of SB-9 were found in *BglI* cleavage of S-C/D as well as of S-H (Fig. 5B). The amount of DNA in band SB-9 in a complete *SalI* + *BglI* digest was greater than the amount in neighboring bands (Fig. 1A and C). SB-9, therefore, was a doublet composed of fragment SB-9a, corresponding to S-H, and fragment SB-9b, contained in S-C or S-D. Both of these fragments (9a and 9b) were obtained from cleavage of B-A plus B-B with *SalI*.

Cleavage map. The analysis described above allowed the determination of positions of all cleavage sites relative to each other and the construction of a cleavage map based on the *SalI* + *KpnI* map previously obtained (4). Cleavage sites surrounding fragments K-F, B-C, B-D, B-E, B-F, and B-G and the position of the *Bam*HI site were unambiguous, since the sizes of the single digest fragments could be calculated directly from their electrophoretic mobility and compared with the sizes of the double digest fragments that they contained. Fragments B-A and B-B were too large for a direct estimate of their size and could not be separated preparatively for unambiguous assignment of subfragments. B-B and SB-3 were both fused to their neighbor (B-F and SB-12, respectively) by the deletion *r*1589 (Fig. 2 and Table 4). Fragments SB-3 and SB-12 together, therefore, made up S-C, which was the *SalI* fragment spanning *r*1589. The size of S-C could then be calculated as the sum of SB-3 plus SB-12, which was 24 kbp. The other *SalI* fragment in the C/D doublet, S-D, therefore contained SB-4 and SB-9b and was slightly smaller. Since B-B extended about 40 kbp clockwise from the *BglI* site under *r*1589 (Table 3), it must have contained SB-3 and the next two *SalI* fragments (I and G, corresponding to SB-7 and SB-11) and a subfragment of about 7 kbp from S-D. The only subfragment shared between B-A and B-B, on the one hand, and S-D, on the other hand, was SB-9b (6.9 kbp [Fig. 5]). Fragments SB-1 (= S-B), SB-9a (= S-H), SB-8, and SB-13, therefore, made up B-A.

Table 5 summarizes the correspondence between fragments from single and double digests of T4 Cyt-0 DNA. *KpnI* + *BglI* subfragments were assigned, based on positions of cleavage sites for the two enzymes as determined above, and verified experimentally for B-C, B-D, B-E, and B-F. Bearing in mind that the most precise size determinations from electrophoretic mobility were obtained for fragments in sizes ranging from about 5 to about 20 kbp, the final positions of cleavage sites were adjusted whenever possible by using fragments in this size range to get from one site to the next. The net distance around the genome, calculated in this way, corresponded to a genome DNA length of 166.5 kbp, which was in good agreement with less direct estimates of the genome length of phage T4 (15).

All cleavage sites were then related to the genetic map, starting at the *BglI* site between B-F and B-B, which was deleted by *r*1589. Pribnow et al. (submitted for publication) have de-

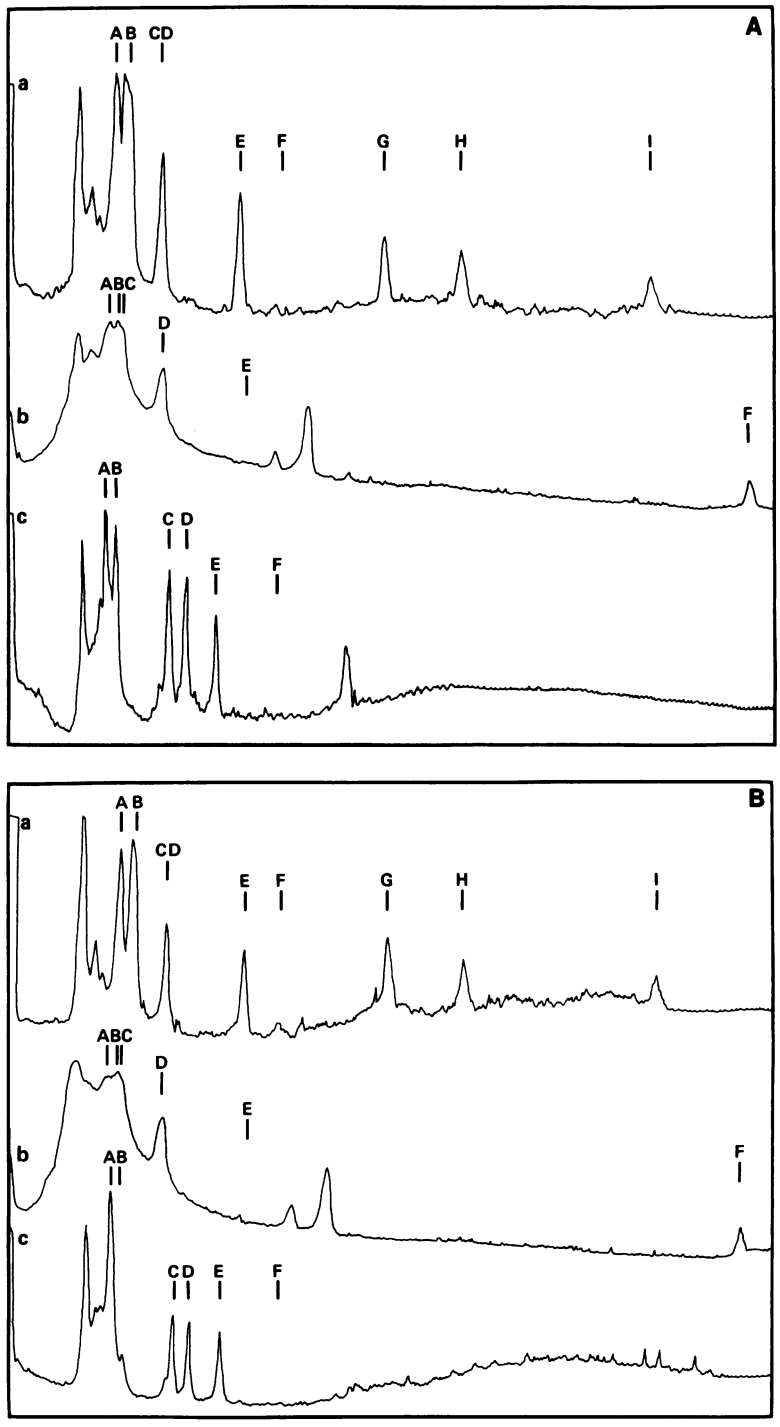

FIG. 2. *Cleavage of T4 DNA containing different deletions. All panels show the following from top to bottom: a, SalI cleavage; b, KpnI cleavage; and c, BglI cleavage. The letters above the tracings indicate the positions of the corresponding bands from digests of Cyt-0 DNA (Fig. 1C). (A) Cyt-9 DNA; (B) Cyt-9,1589 DNA; (C) Cyt-9,12 DNA; and (D) Cyt-9,tk2 DNA. The smallest fragments (B-G and K-G) are usually not included in the figures; they were, however, found in all digests, except for KpnI cleavage of Cyt-9,12 DNA (C, tracing b), where K-G is missing. The unmarked peak near the top of the gel consists of undigested or partially digested DNA.*

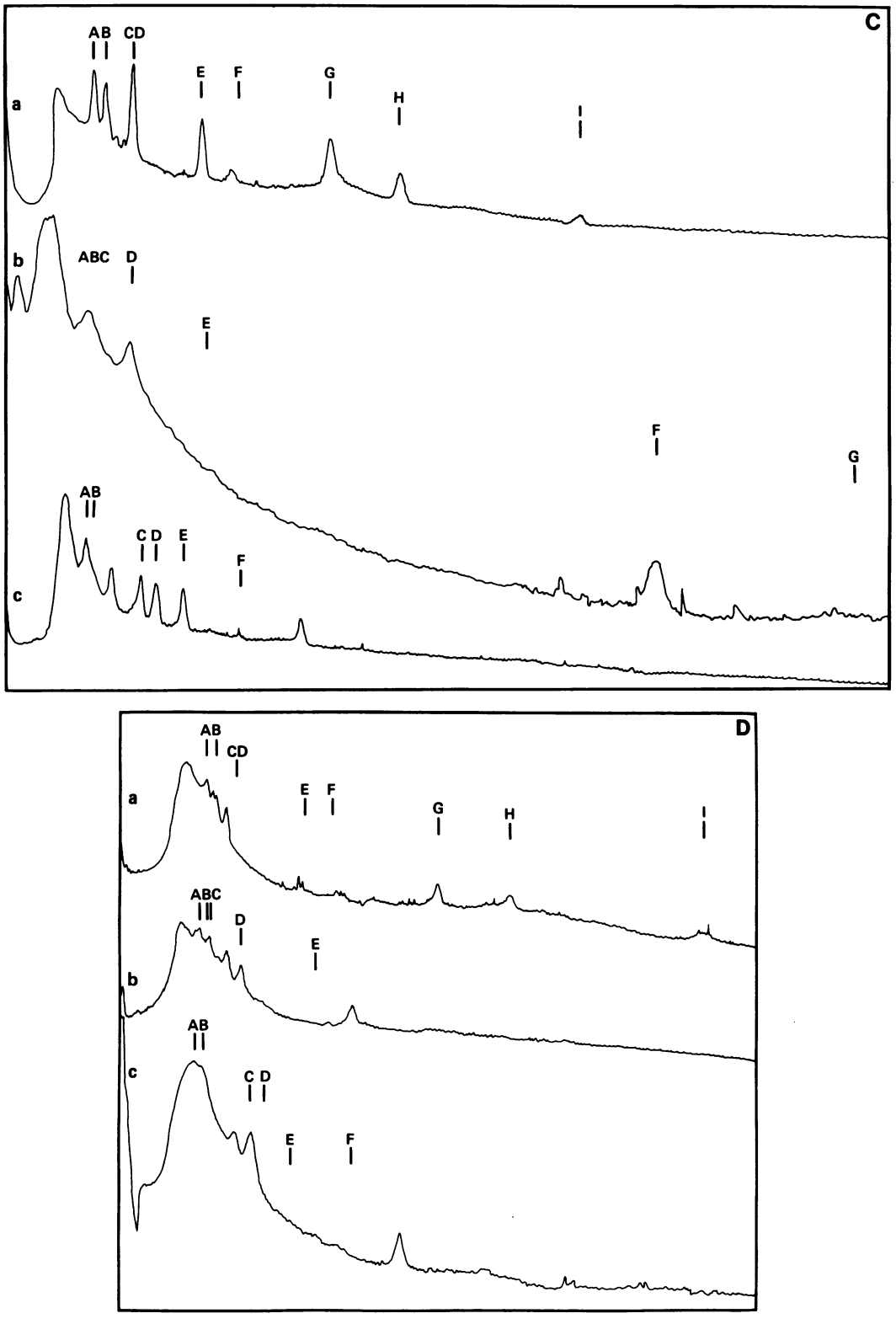

FIG. 2 C and D.

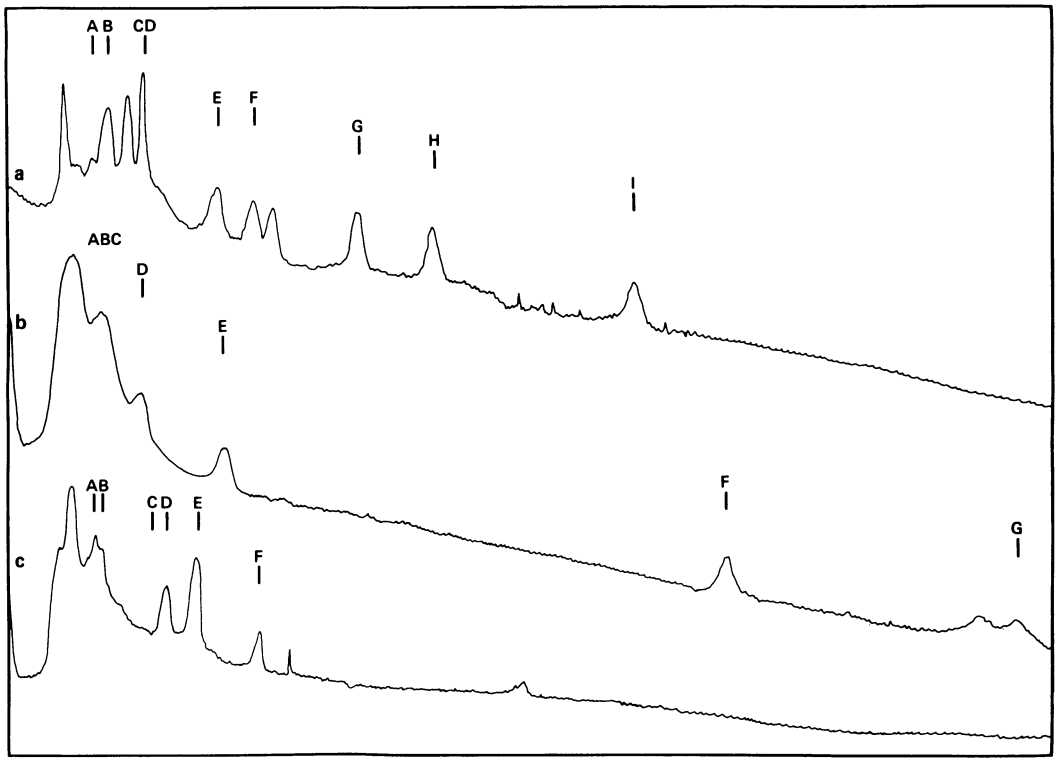

FIG. 3. *Cleavage of Cyt-0 DNA by BamHI in combinations with the following: a, SalI; b, KpnI; or c, BglI. Letters above the tracings identify positions of fragments obtained by cleaving Cyt-0 DNA with SalI, KpnI, or BglI alone (Fig. 1C). Fragment B-G was observed, but was not included in the figure. The unmarked peak near the top of the gel consists of undigested or partially digested DNA.*

termined the nucleotide sequence of a region spanning the *r*IIA/*r*IIB junction. Their sequence data show a *BglI* site located between 19 and 23 base pairs upstream of the *r*IIB translation start codon. I suggest that the first adenine·thymine (A·T) pair in this triplet be used to define the zero point in the genetic and physical maps. This translation start point can be considered an unambiguous definition of "the border between *r*IIA and *r*IIB" commonly employed as a reference point (32). Since genetic map coordinates run clockwise, whereas *r*II is transcribed counterclockwise (32), this A·T pair defines the last nucleotide pair in the map, whereas the nucleotide pair immediately preceding it in the *r*II sense direction defines the first pair (position 1). The *BglI* site between B-F and B-B, therefore, is located between positions 19 and 23 on the physical map.

Coordinates for the cleavage sites for the four enzymes are shown in Fig. 7. Expected sizes for fragments from a triple digest with *SalI* + *KpnI* + *BglI* were calculated from the positions of cleavage sites for these enzymes as shown in Fig. 7 and compared with the sizes of fragments found (Fig. 1A). This comparison (Table 6) yielded good agreement and confirmed the cleavage positions as determined.

Figure 8 shows the cleavage map of T4 thus obtained in relation to the genetic map of this phage. Cleavage maps for *SalI* and *KpnI* were constructed independently by Kiko et al. (14), Rüger et al. (21), O'Farrell et al. (manuscript in preparation), and Marsh (manuscript in preparation). These authors have, in addition, mapped several other enzymes, and the latter two investigators have correlated their maps to the genetic map. These maps are all in very good agreement.

DISCUSSION

Cleavage patterns. The data reported here concern a total of 24 cleavage sites for four sequence-specific endonucleases: 9 sites for *SalI*, 7 sites each for *KpnI* and *BglI*, and 1 site for *Bam*HI. As it was previously (4), I found that complete cleavage of a given batch of DNA could not be achieved simply by increasing the amount of enzyme added. The cleavage patterns illustrated in Fig. 1 through 3 all show the pres-

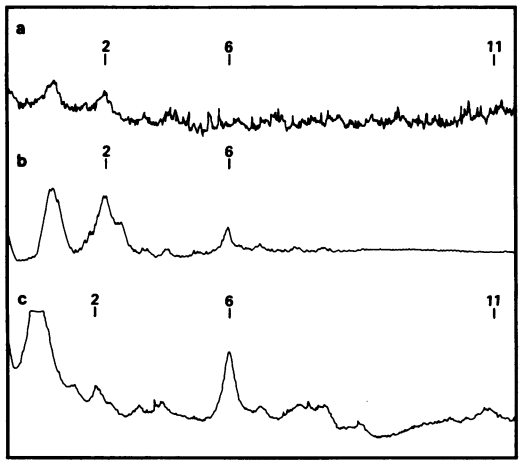

FIG. 4. *Hybridization of the following to SalI + BglI fragments from Cyt-0 DNA: a, K-F; b, SK-13; and c, SK-14. Numbers above the tracings identify the SB fragments. The unmarked peak near the left corresponds to undigested or partially digested DNA.*

ence of small amounts of undigested DNA. They represent limit digest patterns, nevertheless, since the same fragment pattern was observed with various amounts of residual undigested DNA. Cleavage of such undigested DNA extracted from the gels yielded the same fragment patterns as were obtained from unfractionated DNA (data not shown). We previously suggested that these results could be explained if some enzyme molecules bind to a cleavage site without cleaving it (4). If this is the case, this behavior must be random with respect to the cleavage sites studied here (I could not, of course, rule out the possibility that some potential sites were completely protected).

The cleavage patterns seem to be independent of the allelic state of gene *42* (deoxycytidine hydroxymethylase) (Fig. 1 and 2). It is, therefore, rather unlikely that residual hydroxymethylation protects some potential cleavage sites exclusively. Experiments are in progress to test whether bacterium- or phage-coded methylases are involved in protection against cleavage by methylation of adenine or cytosine or both in phage DNA.

Size determinations. The physical map of T4 DNA was constructed from lengths of DNA fragments determined by agarose gel electrophoresis and correlated to the genetic map by analysis of cleavage patterns of several genetically characterized deletion mutants. The accuracy of the constructed map is, of course, crucially dependent upon the precision in size determinations from gel electrophoresis.

The length determinations were based on lengths of DNA fragments from λ or P4 DNA, assuming an inverse relationship between the number of base pairs and the rate of migration (24). Conceivably, the relationship between the size in kbp and the rate of migration could be affected by the average base composition of the DNA, invalidating my use of λ DNA fragments as size standards. However, B. Nordgård in this laboratory (personal communication) has measured the lengths of *SalI* fragments D, E, F, G, H, and I from Cyt-9 DNA by electron microscopy, with results in good agreement with mine. Thus, a change in average base composition from about 65% A·T (T4 [27]) to about 50% A·T (λ [27]) does not seem to affect significantly the mobility of the DNA during electrophoresis.

The positions in Fig. 7, with one exception, were derived from fragments of less than about 20 kbp, within which range the fragment size was inversely proportional to the distance mi-

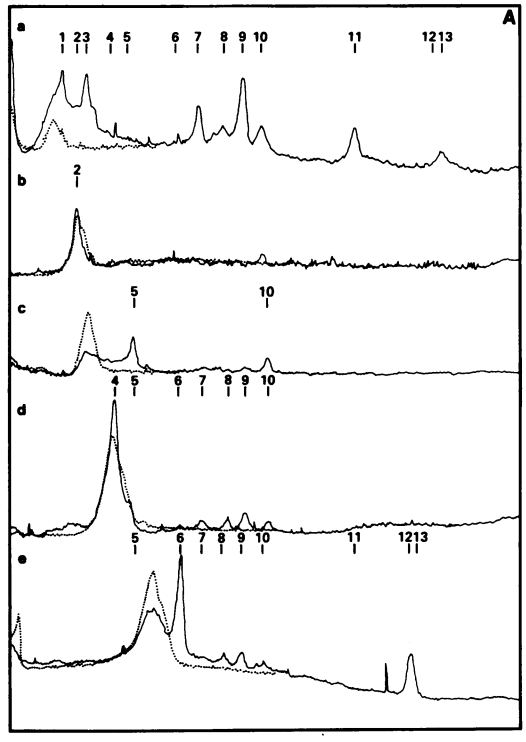

FIG. 5A. *Reciprocal digestion of Cyt-0 DNA with SalI and BglI. (A) BglI fragments eluted, digested with SalI, and electrophoresed. Top to bottom: a, B-A and B-B together; b, B-C; c, B-D; d, B-E; and e, B-F. (B) SalI fragments eluted, digested with BglI, and electrophoresed. Top to bottom: a, S-A; b, S-B; c, S-C/D; d, S-E; and e, S-F. In both (A) and (B), dotted lines show reanalysis of the eluted fragments without further treatment. Positions of the SB fragments are indicated by numbers above the tracings.*

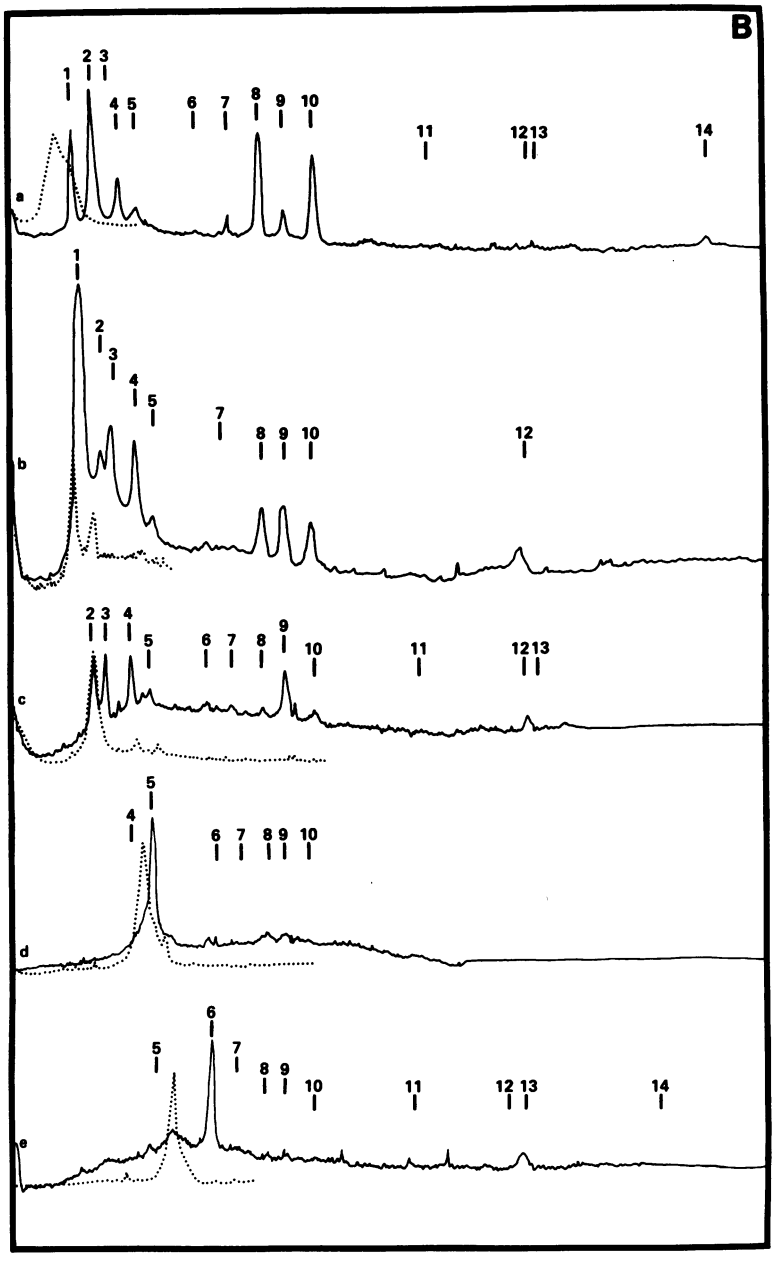

FIG. 5B.

grated under my electrophoretic conditions. The interval from positions 111 to 137 was slightly longer, but contained no cleavage sites for the enzymes studied here. Its length was therefore, somewhat less precise than was the rest of the map. The *SalI-KpnI* fragment spanning this interval (SK-1) was digested with *BglII*, yielding subfragments adding up to 26 kbp, which was in good agreement with the direct estimate (data not shown).

The interval 111 to 137 spans the *alc* gene (22). Its length is calculated to be 25.5 kbp in Cyt-9 DNA (*alc2*) (4) and 26.0 kbp in Cyt-0 DNA (*alc10*) (Table 3). Although these values are not significantly different, I could not at present rule out a small difference between the two strains in this area.

Physical map. The presence of a *BglI* cleav-

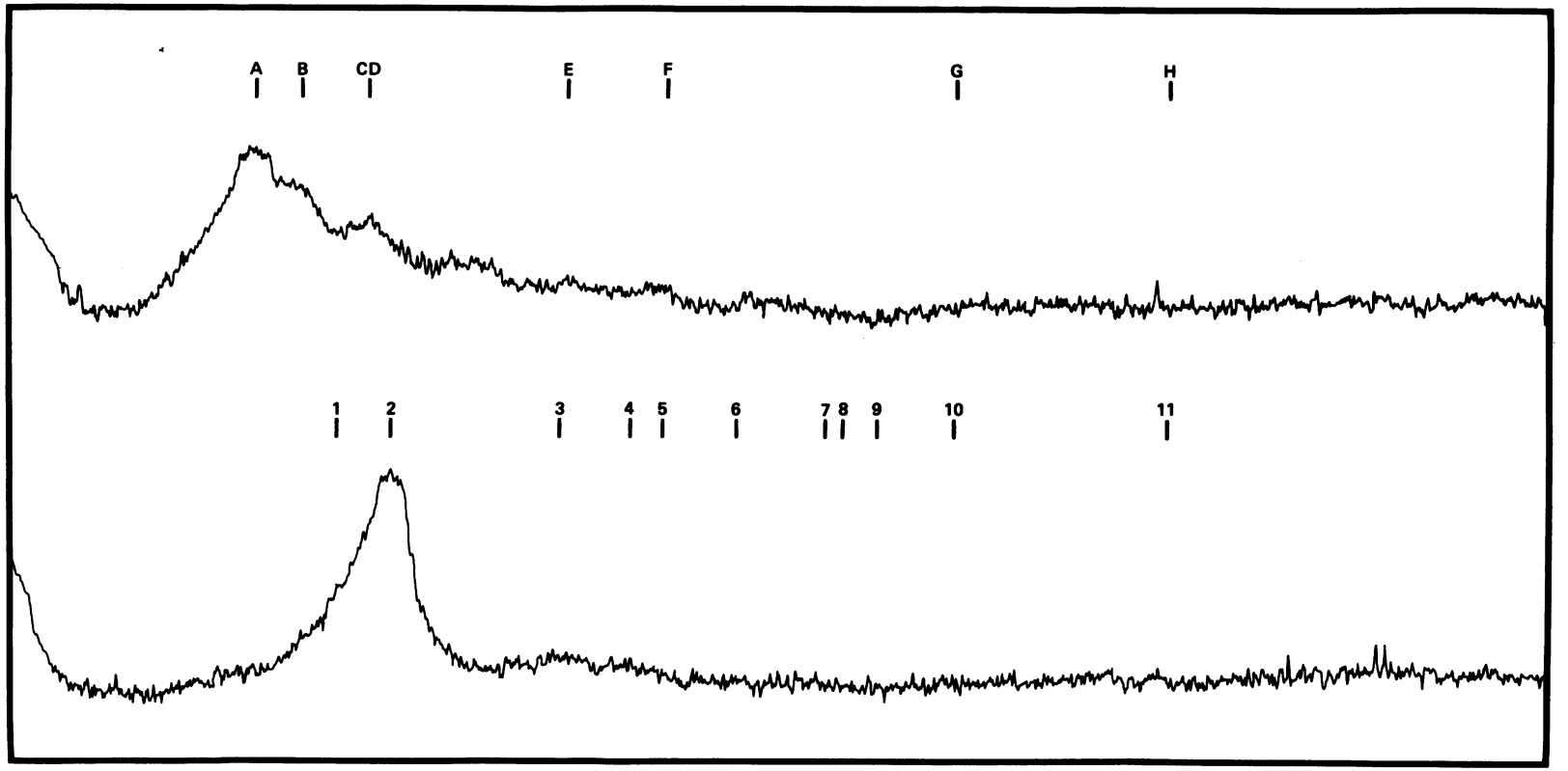

FIG. 6. *Hybridization of B-G to blotted Cyt-0 DNA digested with SalI (top tracing) or with SalI + KpnI (bottom tracing). The positions of S and SK fragments are indicated by letters and numbers above the tracings.*

TABLE 5. *Correspondence between T4 fragments from single and double digests*

Single digest fragment	Fragments from double digests			Single digest fragment size[a]
	SalI + *KpnI*	*SalI* + *BglI*	*KpnI* + *BglI*[b]	
S-A	2, 4, 13	2, 8, 10, 14		38.4
S-B	1, 11b	1		33.3
S-C	6, 8, 15	3, 12		24.0
S-D	5, 7	4, 9b		23.4
S-E	3	5, 15		15.1
S-F	9, 14	6, 13		12.8
S-G	10	7		8.9
S-H	11a	9a		7.0
S-I	12	11		3.9
K-A	1, 2		*1, 5, 14*	48.1
K-B	3, 4, 7		*3, 6, 8*	38.9
K-C	5, 8, 10, 12		*2, 10*	36.5
K-D	9, 11a, 11b		*4, 9*	23.8
K-E	6, 14		*7, 11*	14.6
K-F	13		12	3.2
K-G	15		13	1.6
B-A		1, 8, 9a, 13	*1, 4*	50.8
B-B		3, 7, 9b, 11	*2, 7, 13*	40.9
B-C		2	5, 8, 12	23.2
B-D		5, 10	3	20.3
B-E		4, 15	6, 10	17.3
B-F		6, 12	9, 11	13.0
B-G		14	14	1.2

[a] Size in kbp, calculated from cleavage positions in Fig. 7.

[b] Where italicized, estimated from the calculated cleavage positions for *KpnI* and *BglI* (Fig. 7).

age site within a sequenced region including the origin of the genetic map (Pribnow et al., submitted for publication) permits an exact alignment of physical and genetic maps in this region. Less precise alignments are obtained from the deletion mapping.

The deletion *saΔ9* removes about 2,500 base pairs from *D1* through *stp* (9) between positions 162 and 165 in the genetic map (18, 32). This deletion removes a cleavage site for *SalI* at position 163.7 in the physical map, and its physical size is estimated to be 2.5 kbp. These data are in good agreement.

The deletion *del(39-56)12* (12) is located between gene *39* (position about 3 to 5) and gene *56* (position about 18 to 18.5) (18, 32). The deletion removes two *KpnI* sites at positions 8.8 and 10.3. The distance from *del(39-56)12* to *r1589* was measured by Homyk and Weil (12) by the electron microscope heteroduplex technique. By recalculating their data to λ = 48.3 kbp (26) and using my determinations of endpoints of *r1589* based on the sequence data of Pribnow et al. (submitted for publication) and my estimate of the length of the deletion, *del(39-56)12* could be placed between positions 5.6 and 16.7 on the physical map. These physical endpoints were within the interval between genes *39* and *56* on the genetic map (18, 32). The length of the deletion from my electrophoretic measurements was 11.1 kbp, slightly longer than the 9.8 kbp (10.2 kbp when referred to λ = 48.3 kbp) reported by Homyk and Weil. The discrepancy might be due to the different methods used and the difficulties in obtaining precise lengths of single-stranded DNA by electron microscopy.

The deletion *tk2* inactivates genes *rI* and *tk*. Genetic mapping data of Chace and Hall (5) suggest a deletion of about 8 kbp extending counterclockwise up to *nrdC*. This would give it an approximate position between 50 and 57 in the genetic map (18, 32). I have found evidence for a deletion of 10 kbp removing two cleavage sites at position 57.3 (*SalI*) and position 58.2 (*BglI*) on the physical map. Brooks and Hattman (2) have mapped a gene responsible for phage-induced deoxyadenosine methylase activity (the *dam* gene) between genes *nrdC* and *rI* in the closely related phage T2. Heteroduplex analysis of T2 and T4 DNAs (15) shows that the region from positions 47 to 54 is homologous in these two phages. I measured phage-induced deoxyadenosine methylase activity in cells infected by *tk2* phage and found the level of this

TABLE 6. *Fragments from digestion of Cyt-0 DNA with SalI, KpnI, and BglI together*

Fragment	Size (kbp)	
	Expected[a]	Found[b]
SK-1	26.0	26
SB-5	14.3	15
KB-5	12.9	12.5
SK-7/8	10.6	10.4
SB-6	10.2	10.1
SB-7, SK-10	8.9	8.8
KB-7	8.8	
SB-8	7.9	7.7
KB-8	7.2	7.1
KB-9	7.1	
SB-9a, SK-11a, SB-9b, SK-11b	7.0	6.8
SB-10	6.0	6.1
KB-10	5.9	6.0
SB-11, SK-12	3.9	4.0
KB-12, SK-13	3.2	3.3
SK-14	3.1	3.1
SB-12	2.8	2.8
SB-13	2.6	2.6
SK-15, KB-13	1.6	1.6
SB-14, KB-14	1.2	1.2
SB-15	0.8	0.8

[a] From Fig. 7.

[b] From Fig. 1. Sizes were calculated for the bands observed. Some bands probably contain more than one fragment.

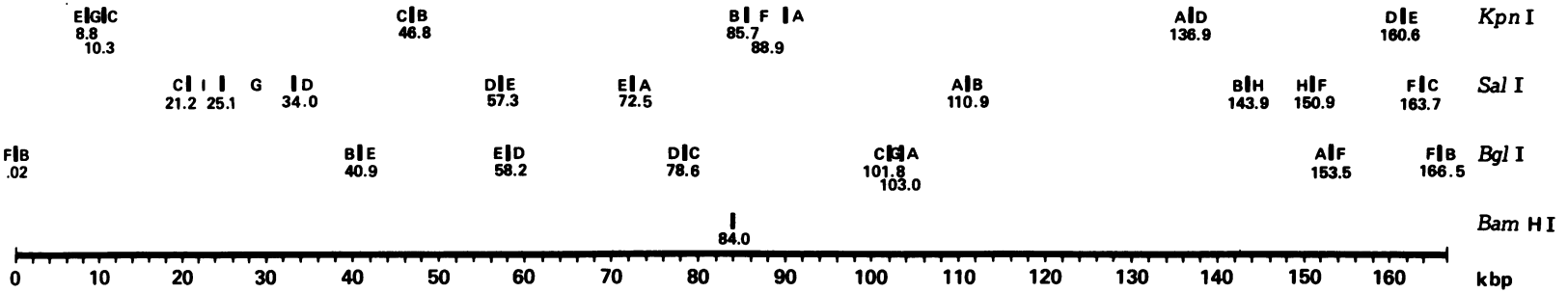

FIG. 7. *Positions of cleavage sites for SalI, KpnI, BglI, and BamHI in T4 Cyt-0 DNA. The locations of the cleavage sites were determined from data in Tables 3, 4, and 5, starting from the BglI site separating B-F from B-B at positions 19 to 23 (Pribnow et al., submitted for publication).*

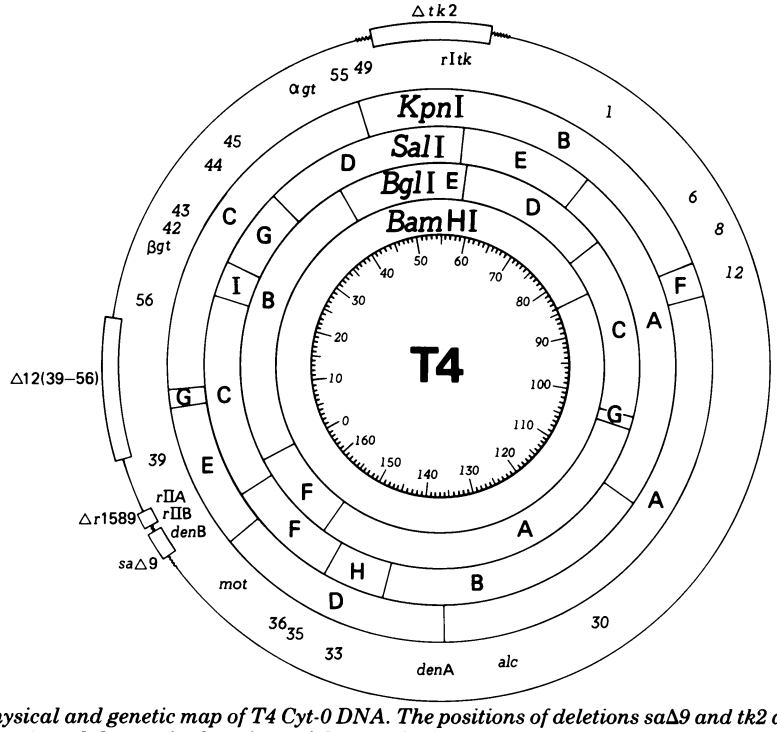

FIG. 8. *Physical and genetic map of T4 Cyt-0 DNA. The positions of deletions saΔ9 and tk2 are from genetic data (5, 9, 18, 31), and the precise locations of these endpoints with respect to the physical map are not known. The endpoints of deletion r1589 were determined from my estimate of its size together with the sequence data of Pribnow et al. (submitted for publication). The position of del(39-56)12 is from electron microscopic determinations of Homyk and Weil relative to r1589 (12), recalculated to a length of lambda DNA of 48.3 kbp (26) which was used in this study, combined with my estimate of the deletion length (Table 4). Estimates of deletion lengths are from Table 4. Positions of genes are from Mosig et al. (18). Cleavage sites for SalI, KpnI, BglI, and BamHI are from Fig. 7.*

activity to be the same as that in cells infected with wild-type phage. Taken together, these data suggest a slight discrepancy between genetic and physical maps in this region, where positions of genetic markers should be moved slightly to fit the physical map.

The *Bam*HI endonuclease was shown by Wilson et al. (30) to cleave in the region of gene *8*. The physical position of the cleavage site, at position 84.0, agrees well with the genetic mapping of gene *8* at position 84 (18).

The fact that relatively few cleavage sites, 24 within 166 kbp, were located in this study precluded a finer alignment of physical and genetic maps. On the other hand, the positions of the cleavage sites themselves should be quite accurate, since the map (with the exception of the one area between positions 111 and 137) was derived by adding lengths of relatively few fragments, the sizes of which were determined with reasonable accuracy. It should therefore provide a solid framework for future, more detailed studies.

ACKNOWLEDGMENTS

I thank D. H. Hall, A. W. Kozinski, E. Kutter, G. Mosig, P. Snustad, and J. Wiberg for gifts of strains and R. Marsh, P. O'Farrell, and D. Pribnow for communicating unpublished data. I am very grateful to L. Korsnes for the P4 DNA and the polyacrylamide gel analysis, to F. Holand, B. Nicolaisen, and A. Øvervatn for their expert assistance with the experimental work, and to C. Linder for his criticism of the manuscript.

This investigation was partially supported by grant C.17.14-51 from the Norwegian Research Council for Science and the Humanities.

LITERATURE CITED

1. **Bertani, G.** 1951. Studies on lysogenesis. I. The mode of phage liberation by lysogenic *Escherichia coli*. J. Bacteriol. **62**:293–300.
2. **Brooks, J., and S. Hattman.** 1973. Location of the DNA-adenine methylase gene on the genetic map of phage T2. Virology **55**:285–288.
3. **Carlson, K., and A. W. Kozinski.** 1974. Nonreplicated DNA and DNA fragments in T4 r⁻ bacteriophage particles: phenotypic mixing of a phage protein. J. Virol. **13**:1274–1290.
4. **Carlson, K., and B. Nicolaisen.** 1979. Cleavage map of bacteriophage T4 cytosine-containing DNA by sequence-specific endonucleases *SalI* and *KpnI*. J. Virol.

31:112-123.
5. **Chace, K. V., and D. H. Hall.** 1975. Characterization of new regulatory mutants of bacteriophage T4. II. New class of mutants. J. Virol. **15**:929-945.
6. **Champe, S. P., and S. Benzer.** 1962. An active cistron fragment. J. Mol. Biol. **4**:228-292.
7. **Denhardt, D.** 1966. A membrane filter technique for the detection of complementary DNA. Biochem. Biophys. Res. Commun. **23**:641-646.
8. **Depew, R. E., and N. R. Cozzarelli.** 1974. Genetics and physiology of bacteriophage T4 3'-phosphatase: evidence for involvement of the enzyme in T4 DNA metabolism. J. Virol. **13**:888-897.
9. **Depew, R. E., T. J. Snopek, and N. R. Cozzarelli.** 1975. Characterization of a new class of deletions of the D region of the bacteriophage T4 genome. Virology **64**: 144-152.
10. **Goldstein, L., M. Thomas, and R. W. Davis.** 1975. *Eco*RI endonuclease cleavage map of bacteriophage P4 DNA. Virology **66**:420-427.
11. **Haggerty, D. M., and R. F. Schleif.** 1976. Location in bacteriophage lambda DNA of cleavage sites of the site-specific endonuclease from *Bacillus amyloliquefaciens* H. J. Virol. **18**:659-663.
12. **Homyk, T., and J. Weil.** 1974. Deletion analysis of two nonessential regions of the T4 genome. Virology **61**: 505-523.
13. **Kahn, M., and A. Hopkins.** 1978. Restriction endonuclease cleavage map of bacteriophage P4 DNA. Virology **85**:359-363.
14. **Kiko, H., E. Niggemann, and W. Rüger.** 1979. Physical mapping of the restriction fragments obtained from bacteriophage T4 dC-DNA with the restriction endonucleases *Sma*I, *Kpn*I, and *Bgl*II. Mol. Gen. Genet. **172**:303-312.
15. **Kim, J. S., and N. Davidson.** 1974. Electron microscope heteroduplex study of sequence relations of T2, T4, and T6 bacteriophage DNAs. Virology **57**:93-111.
16. **Kutter, E., A. Beug, R. Sluss, L. Jensen, and D. Bradley.** 1975. The production of undegraded cytosine-containing DNA by bacteriophage T4 in the absence of dCTPase and endonucleases II and IV, and its effect on protein synthesis. J. Mol. Biol. **99**:591-607.
17. **Maniatis, T., A. Jeffrey, and D. G. Kleid.** 1975. Nucleotide sequence of the rightward operator of phage lambda. Proc. Natl. Acad. Sci. U.S.A. **72**:1184-1188.
18. **Mosig, G., A. Luder, G. Garcia, R. Dannenberg, and S. Bock.** 1978. *In vivo* interaction of genes and proteins in DNA replication and recombination of phage T4. Cold Spring Harbor Symp. Quant. Biol. **43**:501-515.
19. **Murray, K., and N. E. Murray.** 1975. Phage lambda receptor chromosomes for DNA fragments made with restriction endonuclease III of *Haemophilus influenzae* and restriction endonuclease I of *Escherichia coli*. J. Mol. Biol. **98**:551-564.
20. **Peacock, A. C., and C. W. Dingman.** 1967. Resolution of multiple ribonucleic acid species by polyacrylamide gel electrophoresis. Biochemistry **6**:1818-1827.
21. **Rüger, W., M. Neumann, U. Rohr, and E. Niggemann.** 1979. The complete maps of *Bgl*II, *Sal*I, and *Xho*I restriction sites on T4 dC-DNA. Mol. Gen. Genet. **176**:417-425.
22. **Sirotkin, K., J. Wei, and L. Snyder.** 1977. T4 bacteriophage-coded RNA polymerase subunit blocks host transcription and unfolds the host chromosome. Nature (London) **265**:28-32.
23. **Snyder, L., L. Gold, and E. Kutter.** 1976. A gene of bacteriophage T4 whose gene product prevents true late transcription on cytosine-containing DNA. Proc. Natl. Acad. Sci. U.S.A. **73**:3098-3102.
24. **Southern, E. M.** 1975. Detection of specific sequences among DNA fragments separated by gel electrophoresis. J. Mol. Biol. **98**:503-517.
25. **Southern, E.** 1979. Measurements of DNA length by gel electrophoresis. Anal. Biochem. **100**:319-323.
26. **Stüber, D., and H. Bujard.** 1977. Electron microscopy of DNA: determination of absolute molecular weights and linear density. Mol. Gen. Genet. **154**:299-303.
27. **Szybalski, W.** 1968. Use of cesium sulphate for equilibrium density gradient centrifugation. Methods Enzymol. **12**:330-360.
28. **Takahashi, H., M. Shimizu, H. Saito, and Y. Ikeda.** 1979. Studies of viable T4 bacteriophage containing cytosine-substituted DNA (T4 dC-phage). Mol. Gen. Genet. **168**:49-53.
29. **Thomas, M., and R. W. Davis.** 1975. Studies on the cleavage of bacteriophage lambda DNA with *Eco*RI restriction endonuclease. J. Mol. Biol. **91**:315-328.
30. **Wilson, G. G., R. L. Neve, G. J. Edlin, and W. H. Konigsberg.** 1979. The *Bam*HI restriction site in the bacteriophage T4 chromosome is located in or near gene *8*. Genetics **93**:285-296.
31. **Wood, W. B.** 1966. Host specificity of DNA produced by *Escherichia coli*: bacterial mutations affecting the restriction and modification of DNA. J. Mol. Biol. **16**: 118-133.
32. **Wood, W. B., and H. R. Revel.** 1976. The genome of bacteriophage T4. Bacteriol. Rev. **40**:847-868.